

## Photocatalysis

International Edition: DOI: 10.1002/anie.201814265  
German Edition: DOI: 10.1002/ange.201814265ZnSe Nanorods as Visible-Light Absorbers for Photocatalytic and Photoelectrochemical H<sub>2</sub> Evolution in WaterMoritz F. Kuehnel<sup>†</sup>, Charles E. Creissen<sup>†</sup>, Constantin D. Sahn<sup>†</sup>, Dominik Wielend, Anja Schlosser, Katherine L. Orchard, and Erwin Reisner\*

**Abstract:** A precious-metal- and Cd-free photocatalyst system for efficient H<sub>2</sub> evolution from aqueous protons with a performance comparable to Cd-based quantum dots is presented. Rod-shaped ZnSe nanocrystals (nanorods, NRs) with a Ni(BF<sub>4</sub>)<sub>2</sub> co-catalyst suspended in aqueous ascorbic acid evolve H<sub>2</sub> with an activity up to 54 ± 2 mmol<sub>H<sub>2</sub></sub> g<sub>ZnSe</sub><sup>-1</sup> h<sup>-1</sup> and a quantum yield of 50 ± 4% (λ = 400 nm) under visible light illumination (AM 1.5G, 100 mW cm<sup>-2</sup>, λ > 400 nm). Under simulated full-spectrum solar irradiation (AM 1.5G, 100 mW cm<sup>-2</sup>), up to 149 ± 22 mmol<sub>H<sub>2</sub></sub> g<sub>ZnSe</sub><sup>-1</sup> h<sup>-1</sup> is generated. Significant photocorrosion was not noticeable within 40 h and activity was even observed without an added co-catalyst. The ZnSe NRs can also be used to construct an inexpensive delafossite CuCrO<sub>2</sub> photocathode, which does not rely on a sacrificial electron donor. Immobilized ZnSe NRs on CuCrO<sub>2</sub> generate photocurrents of around -10 μA cm<sup>-2</sup> in an aqueous electrolyte solution (pH 5.5) with a photocurrent onset potential of approximately +0.75 V vs. RHE. This work establishes ZnSe as a state-of-the-art light absorber for photocatalytic and photoelectrochemical H<sub>2</sub> generation.

Artificial photosynthesis in which solar energy is stored in chemical fuels is a promising strategy for overcoming the temporal mismatch between renewable energy supply and demand.<sup>[1]</sup> H<sub>2</sub> is the most prominent example of a solar fuel as it can be generated by photoreduction of aqueous protons by a broad range of photocatalysts.<sup>[2]</sup> Among the most active materials are chalcogenide nanocrystals based on CdS and

CdSe.<sup>[3]</sup> Despite the remarkable activities and stabilities shown by these materials,<sup>[4]</sup> the toxicity and carcinogenic nature of cadmium represents a considerable obstacle for their wide-spread application. Carbon-based materials, such as carbon nitride,<sup>[5]</sup> carbon dots,<sup>[6]</sup> and conjugated organic polymers<sup>[7]</sup> have recently been introduced as environmentally benign alternatives. While these materials are inexpensive and usually non-toxic, their performances have yet to match those of Cd-based photocatalysts to achieve high quantum yields for aqueous H<sub>2</sub> production without precious and carcinogenic metals.

Here, we report ZnSe nanorods (NRs) as inexpensive Cd-free light absorbers for efficient H<sub>2</sub> evolution under visible-light irradiation (Figure 1). The ZnSe NRs exhibit an activity approaching that of Cd-based materials, even without an added co-catalyst. Furthermore, we demonstrate that the high activity of the suspended ZnSe nanocrystals under sacrificial conditions can be translated to heterogeneous conditions by assembling a simple, precious-metal-free photoelectrode from ZnSe nanocrystals immobilized on *p*-type delafossite CuCrO<sub>2</sub>.

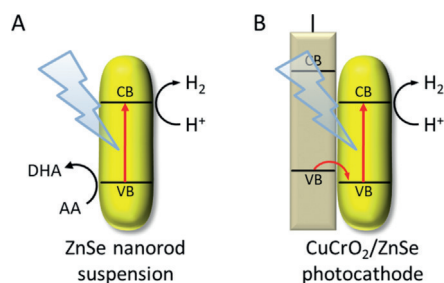


**Figure 1.** Schematic representation of the reported ZnSe nanorod photocatalyst system and its application for the construction of a noble-metal-free photocathode (CB: conduction band, VB: valence band, AA: ascorbic acid, DHA: dehydroascorbic acid).

ZnSe is a stable and inexpensive semiconductor with a direct bulk band gap of 2.7 eV,<sup>[8]</sup> which enables absorption of near-UV and some visible light. The conduction band (CB) is located at around -1.1 V vs. NHE (pH 0),<sup>[9]</sup> providing ample driving force for the reduction of aqueous protons. Despite these favorable properties, ZnSe has received surprisingly little attention for solar fuel generation, unlike its cadmium analogues CdS and CdSe.<sup>[10]</sup> Domen and co-workers reported ZnSe/copper indium gallium selenide (CIGS) solid solution-based photocathodes for H<sub>2</sub> evolution<sup>[11]</sup> with photocurrents up to 12 mA cm<sup>-2</sup> at 0 V vs. the reversible hydrogen electrode (RHE) and onset potentials of

[\*] Dr. M. F. Kuehnel,<sup>[†]</sup> C. E. Creissen,<sup>[†]</sup> C. D. Sahn,<sup>[†]</sup> D. Wielend, A. Schlosser, Dr. K. L. Orchard, Prof. E. Reisner  
Christian Doppler Laboratory for Sustainable Syngas Chemistry,  
Department of Chemistry, University of Cambridge  
Lensfield Road, Cambridge CB2 1EW (UK)  
E-mail: reisner@ch.cam.ac.uk  
Homepage: <http://www-reisner.ch.cam.ac.uk>  
Dr. M. F. Kuehnel<sup>[†]</sup>  
Department of Chemistry, Swansea University  
Singleton Park, Swansea SA2 8PP (UK)

[†] These authors contributed equally to this work.

Supporting information and the ORCID identification number(s) for the author(s) of this article can be found under:  
<https://doi.org/10.1002/anie.201814265>.

Additional data related to this publication are available at the University of Cambridge data repository:  
<https://doi.org/10.17863/CAM.36101>

© 2019 The Authors. Published by Wiley-VCH Verlag GmbH & Co. KGaA. This is an open access article under the terms of the Creative Commons Attribution License, which permits use, distribution and reproduction in any medium, provided the original work is properly cited.

+ 0.89 V vs. RHE.<sup>[11b]</sup> However, the complex photocathode assembly required a CdS charge extraction layer and a Pt proton-reduction catalyst. While a number of reports have demonstrated the application of ZnSe-based nanomaterials for photocatalytic dye degradation<sup>[12]</sup> and water oxidation,<sup>[13]</sup> only a few examples of Cd-free ZnSe particles for photocatalytic H<sub>2</sub> generation have been reported, all of which show low activity.<sup>[14]</sup>

We prepared ZnSe NRs by injecting trioctylphosphine/Se into an octadecane solution of zinc stearate at 300 °C, followed by a 25 min growth period.<sup>[15]</sup> Surface modification of the as-prepared stearate-capped ZnSe NRs (ZnSe-St) was achieved by ligand exchange with mercaptopropionic acid to give water-soluble NRs (ZnSe-MPA) and by reactive ligand removal with [Me<sub>3</sub>O][BF<sub>4</sub>] to give ligand-free NRs (ZnSe-BF<sub>4</sub>).<sup>[16]</sup> Independent of the surface capping, the NRs are 5.2 ± 0.6 nm in diameter and 30.0 ± 4.8 nm long (aspect ratio 5.8 ± 0.9), as determined from transmission electron microscopy (TEM, Figure S1 in the Supporting Information). Powder X-ray diffraction (Figure S1F) shows that the ZnSe NRs are obtained as a mixture of the zinc blende and wurtzite polymorphs, as previously observed with ZnSe nanorods synthesized by hot injection.<sup>[17]</sup> The ZnSe NRs show UV-visible light absorption up to about 440 nm (Figure S2A) and two emission maxima separated by 0.097 eV in their photoluminescence (PL) spectra that can be attributed to differences in the band gaps of the two ZnSe polymorphs (Figure S2B).<sup>[18]</sup> Additional emissions at longer wavelengths likely result from trap states as previously observed with ZnSe nanocrystals.<sup>[16a]</sup> PL is reductively quenched by adding ascorbic acid (AA, Figure S2C,D).

Figure 2 shows that ZnSe NRs are highly active photocatalysts for the reduction of aqueous protons to H<sub>2</sub> under

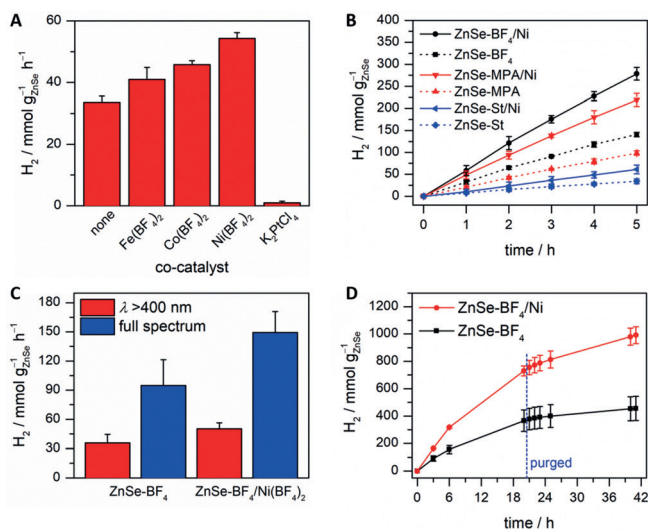


**Figure 2.** Photocatalytic H<sub>2</sub> generation using aqueous ZnSe NRs. A) Ligand-free ZnSe NRs in the presence of different co-catalysts (3 h irradiation). B) Effect of the NR capping ligand. C) ZnSe-BF<sub>4</sub> under different irradiation spectra (1 h irradiation). D) Long-term activity of ZnSe-BF<sub>4</sub> with the photoreactor being purged with N<sub>2</sub> after 20 h. The cumulative amount of H<sub>2</sub> is shown. Conditions unless stated otherwise: 50 mg L<sup>-1</sup> ZnSe NRs, 0.4 M AA, pH 4.5, 20 μM Ni(BF<sub>4</sub>)<sub>2</sub>, 25 °C, 100 mW cm<sup>-2</sup>, AM 1.5G, λ > 400 nm.

visible-light irradiation (AM 1.5G, 100 mW cm<sup>-2</sup>, λ > 400 nm) in the presence of AA. Under optimized conditions (pH 4.5, 0.4 M AA, 50 mg L<sup>-1</sup> ZnSe, see Table S1 and Figure S3 in the Supporting Information for details on optimizing these parameters), ZnSe-BF<sub>4</sub> produced up to 33.6 ± 2.0 mmol<sub>H<sub>2</sub></sub> g<sub>ZnSe</sub><sup>-1</sup> h<sup>-1</sup> (Figure 2A). To further enhance the photocatalytic activity of the ZnSe NRs, Fe(BF<sub>4</sub>)<sub>2</sub>, Co(BF<sub>4</sub>)<sub>2</sub>, Ni(BF<sub>4</sub>)<sub>2</sub>, and K<sub>2</sub>PtCl<sub>4</sub> were tested as co-catalysts (Figure 2A). Ni showed the highest performance increase to 54.3 ± 1.9 mmol<sub>H<sub>2</sub></sub> g<sub>ZnSe</sub><sup>-1</sup> h<sup>-1</sup> at 20 μM, whereas K<sub>2</sub>PtCl<sub>4</sub> quenched the photocatalytic activity almost completely. A low performance of Pt as a co-catalyst has been previously observed with ligand-free CdS.<sup>[19]</sup> Pre-formed Pt nanoparticles showed some activity, but still lower than without a co-catalyst. Under the same conditions, ligand-capped ZnSe-MPA and ZnSe-St NRs showed a lower H<sub>2</sub> generation activity of 45.9 ± 1.4 and 12.1 ± 2.7 mmol<sub>H<sub>2</sub></sub> g<sub>ZnSe</sub><sup>-1</sup> h<sup>-1</sup>, respectively (Figure 2B). This observation agrees with our previous studies, which demonstrated an enhanced H<sub>2</sub> evolution activity of CdS nanocrystals upon ligand removal.<sup>[20]</sup> Under simulated full-spectrum solar irradiation (AM 1.5G, 100 mW cm<sup>-2</sup>), ZnSe-BF<sub>4</sub> generates up to 149 ± 22 mmol<sub>H<sub>2</sub></sub> g<sub>ZnSe</sub><sup>-1</sup> h<sup>-1</sup> and 95 ± 27 mmol<sub>H<sub>2</sub></sub> g<sub>ZnSe</sub><sup>-1</sup> h<sup>-1</sup> in the presence and absence of Ni(BF<sub>4</sub>)<sub>2</sub>, respectively (Figure 2C). The internal quantum yield (IQE) under monochromatic light (λ = 400 nm) was 50.2 ± 3.6% (35.9 ± 2.6% external quantum yield, EQE; Supporting Information, Table S2).

Long-term experiments using ZnSe-BF<sub>4</sub> showed that H<sub>2</sub> production is sustained over more than 40 h with a gradual decrease in rate (Figure 2D). This decreasing activity is likely due to accumulation of dehydroascorbic acid (DHA) in solution. Photodegradation of ZnSe is only marginal, since separating ZnSe-BF<sub>4</sub> NRs after 20 h and re-dispersing them in a fresh AA solution largely restored the activity (some material is lost during separation). In contrast, adding fresh ZnSe NRs had no effect on the activity (Supporting Information, Figure S4). Previous work has shown that the AA oxidation product DHA can inhibit the photocatalytic H<sub>2</sub> production.<sup>[21]</sup> UV/Vis spectra before and after prolonged irradiation show no degradation apart from an increase in scattering resulting from particle aggregation (Figure S5). Post-catalysis TEM confirms the formation of aggregates with aspherical nanocrystalline features (Figure S6). Inductively-coupled plasma optical emission spectroscopy (ICP-OES) of ZnSe-BF<sub>4</sub>/Ni isolated after 3 h irradiation showed an incorporation of 8.5 ± 2.3 Ni atoms per ZnSe NR (< 1% of total added Ni), suggesting in situ formation of a heterogeneous Ni-based catalyst on the NR surface.<sup>[22]</sup> No H<sub>2</sub> was generated without ZnSe, in the dark, or without an electron donor (Supporting Information, Table S3).

These data demonstrate that ZnSe-BF<sub>4</sub> NRs are efficient and stable light absorbers for aqueous H<sub>2</sub> production, considerably outperforming previous Cd-free ZnSe photocatalysts despite their blue-shifted absorption spectrum compared to CdS. Previous reports have shown that a Pt/ZnO-ZnSe nanocomposite generated 3 mmol<sub>H<sub>2</sub></sub> g<sup>-1</sup> h<sup>-1</sup> under UV irradiation with 2.54% EQE,<sup>[14a]</sup> and CoP-decorated ZnSe nanobelts produced < 1 mmol<sub>H<sub>2</sub></sub> g<sup>-1</sup> h<sup>-1</sup> under visible-light irradiation.<sup>[14b]</sup> However, the photocatalytic activities of

ZnSe-BF<sub>4</sub> ( $33.6 \pm 2.0 \text{ mmol}_{\text{H}_2} \text{ g}_{\text{ZnSe}}^{-1} \text{ h}^{-1}$ ,  $25.9 \pm 1.2\%$  EQE) and ZnSe-BF<sub>4</sub>/Ni ( $54.3 \pm 1.9 \text{ mmol}_{\text{H}_2} \text{ g}_{\text{ZnSe}}^{-1} \text{ h}^{-1}$ ,  $35.9 \pm 2.6\%$  EQE) approach those of Cd-based photocatalysts<sup>[23]</sup> such as Cd<sub>0.25</sub>Zn<sub>0.75</sub>Se/CoP ( $45.1 \text{ mmol}_{\text{H}_2} \text{ g}^{-1} \text{ h}^{-1}$ ).<sup>[14b]</sup> CdSe quantum dots (QDs) combined with a Ni catalyst were shown to produce H<sub>2</sub> with an IQE of  $36 \pm 10\%$ .<sup>[24]</sup> Higher performances were reported for CdS with different co-catalysts<sup>[25]</sup> such as MoS<sub>2</sub> ( $96.7 \text{ mmol}_{\text{H}_2} \text{ g}^{-1} \text{ h}^{-1}$ ,  $46.9\%$  EQE),<sup>[25a]</sup> Ni<sub>2</sub>P ( $1200 \text{ mmol}_{\text{H}_2} \text{ g}^{-1} \text{ h}^{-1}$ ,  $41\%$  EQE),<sup>[25b]</sup> and Pt/PdS ( $29.2 \text{ mmol}_{\text{H}_2} \text{ g}^{-1} \text{ h}^{-1}$ ,  $93\%$  EQE).<sup>[25c]</sup> Without a co-catalyst, up to  $41 \text{ mmol}_{\text{H}_2} \text{ g}^{-1} \text{ h}^{-1}$ <sup>[26]</sup> and  $2.8\%$  EQE<sup>[27]</sup> were reported for CdS, and  $239 \text{ mmol}_{\text{H}_2} \text{ g}^{-1} \text{ h}^{-1}$ <sup>[28]</sup> and  $65.7\%$  EQE<sup>[29]</sup> for Cd<sub>x</sub>Zn<sub>1-x</sub>S. Cd-free alternatives such as CuInS<sub>2</sub>-ZnS,<sup>[30]</sup> carbon nitride,<sup>[31]</sup> conjugated polymers,<sup>[32]</sup> triazine frameworks,<sup>[33]</sup> and polymer dots<sup>[34]</sup> generally show much lower activities, although a recently reported NaCl/KCl-treated carbon nitride/Pt material achieved up to  $60\%$  EQE.<sup>[35]</sup>

Having established a good performance and stability of ZnSe nanorods for photocatalytic H<sub>2</sub> production, even in the absence of an added co-catalyst, we aimed to eliminate the sacrificial electron donor AA. The production of low-value H<sub>2</sub> gas at the expense of a sacrificial electron donor is not sustainable unless the electron donor is freely available, for example by photoreforming waste.<sup>[19,36]</sup> Instead, a nanocrystal-sensitized photocathode can be assembled, where the nanocrystal provides electrons for the photocatalysis and a *p*-type semiconductor accepts the photogenerated holes, replacing the chemical electron donor. Such systems enable overall water splitting through coupling with a photoanode for water oxidation.<sup>[37]</sup>

To this end, we immobilized ZnSe-BF<sub>4</sub> NRs on a CuCrO<sub>2</sub> electrode. CuCrO<sub>2</sub> is a wide-band-gap semiconductor ( $E_g \approx 3.1 \text{ eV}$ ), which crystallizes in a delafossite-type structure. Previous work has shown that modification of CuCrO<sub>2</sub> with an organic dye and a nickel bis(diphosphine) catalyst enabled visible-light-driven proton reduction in aqueous solution.<sup>[38]</sup> The characteristic high hole mobility, *p*-type conductivity, and straightforward synthesis from abundant materials using solution processing techniques make CuCrO<sub>2</sub> a suitable candidate for the coupling with ZnSe in a hydrogen-generating photocathode.

The ZnSe nanorods were immobilized by drop-casting ( $8 \mu\text{L cm}^{-2}$ ,  $1.66 \text{ mg mL}^{-1}$ , acetonitrile) directly onto CuCrO<sub>2</sub> electrodes (thickness approx. 300 nm, see Figure S7 in the Supporting Information;  $13.4 \mu\text{g ZnSe cm}^{-2}$ ). EDX spectra confirmed an even distribution over the electrode surface (Figure S8). UV/Vis spectra of ZnSe-modified CuCrO<sub>2</sub> feature the characteristic absorptions of both CuCrO<sub>2</sub> and ZnSe (Figure S9). Linear-sweep voltammograms and chronoamperograms of ZnSe-modified electrodes show enhanced photocurrents compared to the bare CuCrO<sub>2</sub> electrode, with an onset potential of approximately  $+0.75 \text{ V vs. RHE}$  (Figure 3), indicating the ability of photoexcited ZnSe nanorods to inject holes ( $E_{\text{VB,ZnSe}} = 1.6 \text{ V vs. RHE}$ ) into the valence band of CuCrO<sub>2</sub> ( $E_{\text{VB,CuCrO}_2} = 1.0 \text{ V vs. RHE}$ ).<sup>[38]</sup> Controlled potential photoelectrolysis (CPPE; Supporting Information, Figure S10) confirmed that the highly reducing CB<sub>ZnSe</sub> electrons are used to reduce aqueous protons to H<sub>2</sub>. CPPE with a CuCrO<sub>2</sub>|ZnSe electrode maintained at  $E_{\text{app}} = 0 \text{ V vs.}$

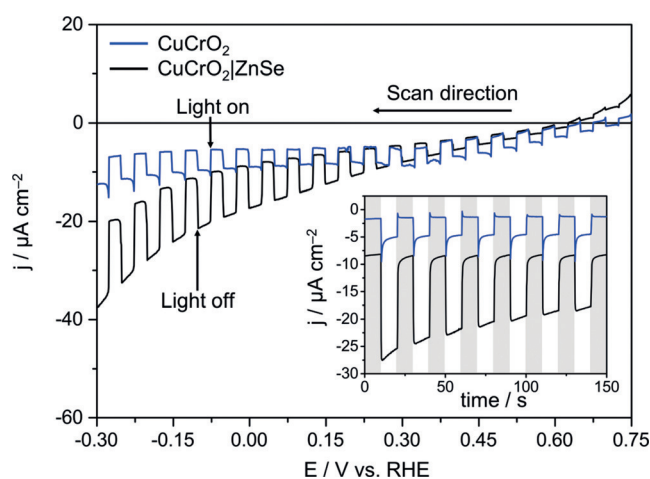


**Figure 3.** Linear-sweep voltammograms under chopped light illumination for CuCrO<sub>2</sub> (blue) and CuCrO<sub>2</sub>|ZnSe (black) electrodes, and chronoamperograms (inset) of the same electrodes at  $E_{\text{app}} = 0 \text{ V vs. RHE}$ . Shading indicates dark chops. Conditions: Aq. Na<sub>2</sub>SO<sub>4</sub> (0.1 M, pH 5.5), room temperature,  $100 \text{ mW cm}^{-2}$ , AM 1.5G,  $\lambda > 400 \text{ nm}$ , scan rate  $5 \text{ mV s}^{-1}$ . The photocurrent density was adjusted for an electrode area of  $0.25 \text{ cm}^2$ .

RHE and illuminated from the front side ( $100 \text{ mW cm}^{-2}$ , AM 1.5G,  $\lambda > 400 \text{ nm}$ ) produced  $35 \pm 7 \text{ nmol H}_2$  over the course of 4 h with a Faradaic efficiency (FE) of  $7 \pm 2\%$  (Table S5). Bare CuCrO<sub>2</sub> produced no detectable H<sub>2</sub>, confirming the essential role of ZnSe in this system. The high dark current, as previously reported for CuCrO<sub>2</sub>,<sup>[38]</sup> and dissolved H<sub>2</sub> which is not sufficiently accounted for in low current-generating systems<sup>[39]</sup> both contribute to the modest FE. Adding Ni<sup>2+</sup> as a co-catalyst increases the overall H<sub>2</sub> production yield, corresponding well to photocatalysis results (Supporting Information, Figure S11 and Table S5). Incident photon-to-current efficiency measurements showed an increased current in the 400–440 nm region for CuCrO<sub>2</sub>|ZnSe electrodes compared to bare CuCrO<sub>2</sub>, confirming the role of ZnSe NRs in this photocathode (Figure S12).

H<sub>2</sub>-generating QD-sensitized photocathodes in the absence of a co-catalyst have shown photocurrents of  $-60 \mu\text{A cm}^{-2}$  at  $0.3 \text{ V vs. RHE}$  with mercaptoacetic-acid-modified CdSe on NiO<sup>[40]</sup> and  $-180 \mu\text{A cm}^{-2}$  at  $0.5 \text{ V vs. RHE}$  using a phenothiazine hole-accepting ligand with CdSe on NiO.<sup>[41]</sup> CuCrO<sub>2</sub>|ZnSe photoelectrodes generated  $-10 \mu\text{A cm}^{-2}$  at  $0 \text{ V vs. RHE}$ , comparable to the photocurrents observed with a molecular dye/catalyst assembly.<sup>[38]</sup> The low photocurrent can be partly attributed to low light absorption, but the dominant limiting factor is likely a non-ideal interface between CuCrO<sub>2</sub> and the ZnSe NRs. This results in high charge recombination, limiting the number of electrons available for catalysis. Adding a H<sub>2</sub> evolution co-catalyst therefore only results in a small activity enhancement. Although this performance does not match that of the corresponding Cd-based systems yet, it does demonstrate that the ZnSe NR photocatalyst can operate in the absence of a sacrificial reagent and in a photoelectrochemical cell. We expect future improvements for the integration of ZnSe into



electrodes through CuCrO<sub>2</sub> nanostructuring and ligand engineering to improve the CuCrO<sub>2</sub>/ZnSe interface,<sup>[40–42]</sup> alternative assembly methods,<sup>[43]</sup> and the integration of molecular catalysts,<sup>[44]</sup> especially for CO<sub>2</sub> reduction,<sup>[16a]</sup> making use of the highly reducing CB of ZnSe.

In summary, we have demonstrated that ZnSe nanorods are efficient light-absorbers for solar-driven H<sub>2</sub> production, even without an added hydrogen-evolution co-catalyst. Their performance already approaches that of Cd-containing quantum dots without exhibiting their carcinogenicity, highlighting the potential of designing novel inorganic materials for efficient photocatalysis. We showed that the ZnSe nanorods can also be integrated into photoelectrochemical cells, which paves the way to closed-cycle solar fuel synthesis and we also envision its use in organic photoredox catalysis and photo-reforming of waste and pollutants in future development.

### Acknowledgements

This work was supported by the Christian Doppler Research Association (Austrian Federal Ministry of Science, Research and Economy and the National Foundation for Research, Technology and Development), the OMV Group (M.F.K., C.D.S., and E.R.), the EPSRC NanoDTC in Cambridge (EP/L015978/1; E.R. and C.E.C.), an EPSRC Underpinning Multi-User Equipment Grant (EP/P030467/1), the Erasmus + program (D.W.), the Erasmus program (A.S.) and the World Premier International Research Center Initiative, MEXT, Japan (K.L.O.). We thank Dr. Jane Leung, Miss Taylor Uekert, and Dr. Nikolay Kornienko for helpful discussions, and Dr. Heather Greer for help with the TEM measurements.

### Conflict of interest

The authors declare no conflict of interest.

**Keywords:** delafossite · hydrogen · photocatalysis · photocathode · zinc selenide

**How to cite:** *Angew. Chem. Int. Ed.* **2019**, *58*, 5059–5063  
*Angew. Chem.* **2019**, *131*, 5113–5117

- [1] Y. Tachibana, L. Vayssieres, J. R. Durrant, *Nat. Photonics* **2012**, *6*, 511–518.
- [2] S. Chen, T. Takata, K. Domen, *Nat. Rev. Mats.* **2017**, *2*, 17050.
- [3] X.-B. Li, C.-H. Tung, L.-Z. Wu, *Nat. Rev. Chem.* **2018**, *2*, 160–173.
- [4] D. W. Wakerley, K. H. Ly, N. Kornienko, K. L. Orchard, M. F. Kuehnel, E. Reisner, *Chem. Eur. J.* **2018**, *24*, 18385–18388.
- [5] W.-J. Ong, L.-L. Tan, Y. H. Ng, S.-T. Yong, S.-P. Chai, *Chem. Rev.* **2016**, *116*, 7159–7329.
- [6] G. A. M. Hutton, B. C. M. Martindale, E. Reisner, *Chem. Soc. Rev.* **2017**, *46*, 6111–6123.
- [7] L. Wang, Y. Zhang, L. Chen, H. Xu, Y. Xiong, *Adv. Mater.* **2018**, *30*, 1801955.
- [8] A. Ebina, E. Fukunaga, T. Takahashi, *Phys. Rev. B* **1974**, *10*, 2495–2500.
- [9] H. Kaneko, T. Minegishi, M. Nakabayashi, N. Shibata, Y. Kuang, T. Yamada, K. Domen, *Adv. Funct. Mater.* **2016**, *26*, 4570–4577.
- [10] Y. Xu, Y. Huang, B. Zhang, *Inorg. Chem. Front.* **2016**, *3*, 591–615.
- [11] a) Y. Kageshima, T. Minegishi, Y. Goto, H. Kaneko, K. Domen, *Sustainable Energy Fuels* **2018**, *2*, 1957–1965; b) H. Kaneko, T. Minegishi, M. Nakabayashi, N. Shibata, K. Domen, *Angew. Chem. Int. Ed.* **2016**, *55*, 15329–15333.
- [12] a) S. Xiong, B. Xi, C. Wang, G. Xi, X. Liu, Y. Qian, *Chem. Eur. J.* **2007**, *13*, 7926–7932; b) L. Zhang, H. Yang, J. Yu, F. Shao, L. Li, F. Zhang, H. Zhao, *J. Phys. Chem. C* **2009**, *113*, 5434–5443; c) T. Yao, Q. Zhao, Z. Qiao, F. Peng, H. Wang, H. Yu, C. Chi, J. Yang, *Chem. Eur. J.* **2011**, *17*, 8663–8670; d) P. Chen, T.-Y. Xiao, H.-H. Li, J.-J. Yang, Z. Wang, H.-B. Yao, S.-H. Yu, *ACS Nano* **2012**, *6*, 712–719; e) S. Cho, J.-W. Jang, J. S. Lee, K.-H. Lee, *Nanoscale* **2012**, *4*, 2066–2071; f) B. Liu, L. Tian, Y. Wang, *ACS Appl. Mater. Interfaces* **2013**, *5*, 8414–8422; g) W. Chen, N. Zhang, M. Y. Zhang, X. T. Zhang, H. Gao, J. Wen, *CrystEngComm* **2014**, *16*, 1201–1206; h) M. B. Tabar, S. M. Elahi, M. Ghoranneviss, R. Yousefi, *CrystEngComm* **2018**, *20*, 4590–4599; i) X. Huang, Y. Zou, J. Hao, J. Jiang, *CrystEngComm* **2018**, *20*, 4020–4024; j) R. Yousefi, H. R. Azimi, M. R. Mahmoudian, W. J. Basirun, *Appl. Surf. Sci.* **2018**, *435*, 886–893.
- [13] D. Chen, H. Zhang, Y. Li, Y. Pang, Z. Yin, H. Sun, L.-C. Zhang, S. Wang, M. Saunders, E. Barker, G. Jia, *Adv. Mater.* **2018**, *30*, 1803351.
- [14] a) A. F. Shaikh, S. S. Arbuj, M. S. Tamboli, S. D. Naik, S. B. Rane, B. B. Kale, *ChemistrySelect* **2017**, *2*, 9174–9180; b) B. Qiu, Q. Zhu, M. Xing, J. Zhang, *Chem. Commun.* **2017**, *53*, 897–900.
- [15] P. Reiss, G. Quemard, S. Carayon, J. Bleuse, F. Chandezon, A. Pron, *Mater. Chem. Phys.* **2004**, *84*, 10–13.
- [16] a) M. F. Kuehnel, C. D. Sahn, G. Neri, J. R. Lee, K. L. Orchard, A. J. Cowan, E. Reisner, *Chem. Sci.* **2018**, *9*, 2501–2509; b) E. L. Rosen, R. Buonsanti, A. Llordes, A. M. Sawvel, D. J. Milliron, B. A. Helms, *Angew. Chem. Int. Ed.* **2012**, *51*, 684–689.
- [17] P. D. Cozzoli, L. Manna, M. L. Curri, S. Kudera, C. Giannini, M. Striccoli, A. Agostiano, *Chem. Mater.* **2005**, *17*, 1296–1306.
- [18] C.-Y. Yeh, S.-H. Wei, A. Zunger, *Phys. Rev. B* **1994**, *50*, 2715–2718.
- [19] D. W. Wakerley, M. F. Kuehnel, K. L. Orchard, K. H. Ly, T. E. Rosser, E. Reisner, *Nat. Energy* **2017**, *2*, 17021.
- [20] C. M. Chang, K. L. Orchard, B. C. M. Martindale, E. Reisner, *J. Mater. Chem. A* **2016**, *4*, 2856–2862.
- [21] a) M. Guttentag, A. Rodenberg, R. Kopelent, B. Probst, C. Buchwalder, M. Brandstätter, P. Hamm, R. Alberto, *Eur. J. Inorg. Chem.* **2012**, 59–64; b) B. C. M. Martindale, E. Joliat, C. Bachmann, R. Alberto, E. Reisner, *Angew. Chem. Int. Ed.* **2016**, *55*, 9402–9406.
- [22] T. Simon, N. Bouchonville, M. J. Berr, A. Vaneski, A. Adrović, D. Volbers, R. Wyrwich, M. Döblinger, A. S. Susha, A. L. Rogach, F. Jäckel, J. K. Stolarczyk, J. Feldmann, *Nat. Mater.* **2014**, *13*, 1013–1018.
- [23] Y.-J. Yuan, D. Chen, Z.-T. Yu, Z.-G. Zou, *J. Mater. Chem. A* **2018**, *6*, 11606–11630.
- [24] Z. Han, F. Qiu, R. Eisenberg, P. L. Holland, T. D. Krauss, *Science* **2012**, *338*, 1321–1324.
- [25] a) J. He, L. Chen, F. Wang, Y. Liu, P. Chen, C.-T. Au, S.-F. Yin, *ChemSusChem* **2016**, *9*, 624–630; b) Z. Sun, H. Zheng, J. Li, P. Du, *Energy Environ. Sci.* **2015**, *8*, 2668–2676; c) H. Yan, J. Yang, G. Ma, G. Wu, X. Zong, Z. Lei, J. Shi, C. Li, *J. Catal.* **2009**, *266*, 165–168; d) M. Gopannagari, D. P. Kumar, D. A. Reddy, S. Hong, M. I. Song, T. K. Kim, *J. Catal.* **2017**, *351*, 153–160; e) Z. Sun, Q. Yue, J. Li, J. Xu, H. Zheng, P. Du, *J. Mater. Chem. A* **2015**, *3*, 10243–10247.
- [26] Y. Xu, W. Zhao, R. Xu, Y. Shi, B. Zhang, *Chem. Commun.* **2013**, *49*, 9803–9805.
- [27] C. Li, L. Han, R. Liu, H. Li, S. Zhang, G. Zhang, *J. Mater. Chem.* **2012**, *22*, 23815–23820.

- [28] D. Jiang, Z. Sun, H. Jia, D. Lu, P. Du, *J. Mater. Chem. A* **2016**, *4*, 675–683.
- [29] H. Du, K. Liang, C.-Z. Yuan, H.-L. Guo, X. Zhou, Y.-F. Jiang, A.-W. Xu, *ACS Appl. Mater. Interfaces* **2016**, *8*, 24550–24558.
- [30] M. Sandroni, R. Gueret, K. D. Wegner, P. Reiss, J. Fortage, D. Aldakov, M.-N. Collomb, *Energy Environ. Sci.* **2018**, *11*, 1752–1761.
- [31] a) Y. Wang, M. K. Bayazit, S. J. A. Moniz, Q. Ruan, C. C. Lau, N. Martsinovich, J. Tang, *Energy Environ. Sci.* **2017**, *10*, 1643–1651; b) M. Z. Rahman, P. C. Tapping, T. W. Kee, R. Smernik, N. Spooner, J. Moffatt, Y. Tang, K. Davey, S.-Z. Qiao, *Adv. Funct. Mater.* **2017**, *27*, 1702384; c) A. Indra, A. Acharjya, P. W. Menezes, C. Merschjann, D. Hollmann, M. Schwarze, M. Aktas, A. Friedrich, S. Lochbrunner, A. Thomas, M. Driess, *Angew. Chem. Int. Ed.* **2017**, *56*, 1653–1657.
- [32] a) R. S. Sprick, B. Bonillo, R. Clowes, P. Guiglion, N. J. Brownbill, B. J. Slater, F. Blanc, M. A. Zwijnenburg, D. J. Adams, A. I. Cooper, *Angew. Chem. Int. Ed.* **2016**, *55*, 1792–1796; b) D. J. Woods, R. S. Sprick, C. L. Smith, A. J. Cowan, A. I. Cooper, *Adv. Energy Mater.* **2017**, *7*, 1700479.
- [33] a) S. Bi, Z.-A. Lan, S. Paasch, W. Zhang, Y. He, C. Zhang, F. Liu, D. Wu, X. Zhuang, E. Brunner, X. Wang, F. Zhang, *Adv. Funct. Mater.* **2017**, *27*, 1703146; b) S. Kuecken, A. Acharjya, L. Zhi, M. Schwarze, R. Schomäcker, A. Thomas, *Chem. Commun.* **2017**, *53*, 5854–5857.
- [34] L. Wang, R. Fernández-Terán, L. Zhang, D. L. A. Fernandes, L. Tian, H. Chen, H. Tian, *Angew. Chem. Int. Ed.* **2016**, *55*, 12306–12310.
- [35] G. Zhang, L. Lin, G. Li, Y. Zhang, A. Savateev, S. Zafeiratos, X. Wang, M. Antonietti, *Angew. Chem. Int. Ed.* **2018**, *57*, 9372–9376.
- [36] a) T. Uekert, M. F. Kuehnel, D. W. Wakerley, E. Reisner, *Energy Environ. Sci.* **2018**, *11*, 2853–2857; b) M. F. Kuehnel, E. Reisner, *Angew. Chem. Int. Ed.* **2018**, *57*, 3290–3296.
- [37] E. A. Gibson, *Chem. Soc. Rev.* **2017**, *46*, 6194–6209.
- [38] C. E. Creissen, J. Warnan, E. Reisner, *Chem. Sci.* **2018**, *9*, 1439–1447.
- [39] C. D. Windle, J. Massin, M. Chavarot-Kerlidou, V. Artero, *Dalton Trans.* **2018**, *47*, 10509–10516.
- [40] B. Liu, X.-B. Li, Y.-J. Gao, Z.-J. Li, Q.-Y. Meng, C.-H. Tung, L.-Z. Wu, *Energy Environ. Sci.* **2015**, *8*, 1443–1449.
- [41] X.-B. Li, B. Liu, M. Wen, Y.-J. Gao, H.-L. Wu, M.-Y. Huang, Z.-J. Li, B. Chen, C.-H. Tung, L.-Z. Wu, *Adv. Sci.* **2016**, *3*, 1500282.
- [42] M. Abdellah, S. Zhang, M. Wang, L. Hammarström, *ACS Energy Lett.* **2017**, *2*, 2576–2580.
- [43] H. Lv, C. Wang, G. Li, R. Burke, T. D. Krauss, Y. Gao, R. Eisenberg, *Proc. Natl. Acad. Sci. USA* **2017**, *114*, 11297–11302.
- [44] a) P. Meng, M. Wang, Y. Yang, S. Zhang, L. Sun, *J. Mater. Chem. A* **2015**, *3*, 18852–18859; b) M. F. Kuehnel, K. L. Orchard, K. E. Dalle, E. Reisner, *J. Am. Chem. Soc.* **2017**, *139*, 7217–7223.

Manuscript received: December 15, 2018

Revised manuscript received: February 2, 2019

Accepted manuscript online: February 4, 2019

Version of record online: March 6, 2019